Reliability Engineering and System Safety 235 (2023) 109263

Contents lists available at ScienceDirect

Reliability Engineering and System Safety

journal homepage: www.elsevier.com/locate/ress

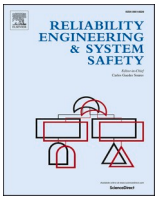

A decision-making approach for the health-aware energy management of ship hybrid power plants

Charalampos Tsoumpris *, Gerasimos Theotokatos

Maritime Safety Research Centre, Department of Naval Architecture, Ocean & Marine Engineering, University of Strathclyde, United Kingdom of Great Britain and Northern Ireland, Glasgow, United Kingdom

ARTICLE INFO

Keywords:
Hybrid power plant
System reliability
Energy management
Dynamic bayesian network
Autonomous operations

ABSTRACT

Although autonomous shipping has attracted increasing interest, its further development requires innovative solutions to operate autonomous ships without the direct intervention of human operators. This study aims to develop a health-aware energy management (HAEM) approach for ship hybrid power plants, integrating the health monitoring information from reliability tools with the energy management tools. This approach employs the equivalent consumption minimisation strategy (ECMS) along with a Dynamic Bayesian network (DBN), as well as the utopia decision-making method and a model for the ship hybrid power plant. The HAEM approach is demonstrated for a parallel hybrid power plant of a pilot boat considering realistic operating profiles. The results demonstrate that by employing HAEM approach for the investigated ship power plant operating for 300 h reduces its failure rate almost fourfold at the cost of fuel consumption increase of around 1.5%, compared to the respective operation with the ECMS. This study is expected to contribute towards the development of supervisory control of autonomous power plants.

1. Introduction

Initiatives to develop autonomous ships have been pursued including research and industrial projects, with the most notable examples of the AUTOSHIP, MUNIN, AAWA, and Yara Birkeland [1,2]. The use of smart sensors, intelligent monitoring capabilities, autonomous decision-making functions and data exchange with wireless connectivity to the shore are constituent parts of the successful autonomous ships operation [3,4]. Nonetheless, technological maturity is not yet achieved, since new technologies are currently being developed and tested [3,5]. As a result, further developments are required, especially for the highly automated parts that must be operated without crew intervention [6].

The ship power plant is an essential part of the autonomous ship, as it provides power to satisfy the ship's propulsive and electrical power demand. However, in the case of autonomous operations, the power plant's requirements are intrinsically different from conventional ships, as the crew cannot perform corrective actions [7]. The system must exhibit sufficient resilience where unexpected events and failures occur, whilst ensuring the system's safe operation [7,8]. In this respect, the system must possess the capability of recovering during disrupting events [9]. Consequently, the availability of the power plant functionality is ranked as a higher priority during the design process and the autonomous operations [10].

Since maintenance in the autonomous ship power plant cannot be performed onboard, it is considered a non-repairable system throughout the sailing phase [11]. Consequently, one of the most crucial requirements for autonomous operation is to preserve the components and system reliability [12]. As the system reliability is greatly influenced by the components' reliability and the power plant's topology, it can be considerably improved by employing configurations with multiple components and redundancy [13]. Hence, the hybrid configurations are expected to attract the autonomous ship designers interest, as they combine both mechanical and electrical components [3,14]. Hybrid power plants contribute to potential fuel savings and emissions reductions, whilst offering redundancy by having multiple power sources and power consumers, thus providing increased system reliability [15,16].

Furthermore, the power plant components operating regions can greatly influence future degradation patterns (typically, operation close to permissible limits accelerates degradation) [17,18]. For configurations with multiple components, the energy management strategies determining the components' setpoints should consider both performance criteria (i.e., fuel consumption) and the health state, to reduce

* Corresponding author.
E-mail address: charalampos.tsoumpris@strath.ac.uk (C. Tsoumpris).

https://doi.org/10.1016/j.ress.2023.109263
Received 18 October 2022; Received in revised form 14 March 2023; Accepted 17 March 2023
Available online 20 March 2023

Nomenclature list

I	current [A]
k_p	propeller constant [–]
l	component load fraction [–]
l_{limit}	maximum engine load at torque/speed limit curve [–]
m	flow mass rate [kg/s]
N	rotational speed [rev/m]
P	power [W]
Q_{LHV}	lower heating value of fuel at ISO conditions [kJ/kg]
Q_{max}	battery capacity [Ah]
R	reliability [–]
R_0	series resistance [Ω]
s	equivalance factor
SOC	state of Charge [–]
t	time [s]
T_s	sampling interval [s]
u	control variable
V_{oc}	open circuit voltage [V]

Greek symbols

β	Weibull distribution shape factor [–]
η	efficiency [–]
λ	failure rate [h^{-1}]

Subscripts

bat	battery
elec	electrical
em	electric machine
eng	engine
eqv	equivalent
f	fuel
i	component identifier
max	maximum
mean	mean
min	minimum
prop	propeller
ress	rechargeable energy storage system
t	target

Abbreviation list

BN	Bayesian network
BSFC	brake-specific fuel consumption
CPT	conditional probabilities tables
DBN	dynamic Bayesian network
DP	dynamic programming
ECMS	equivalent consumption minimisation strategy
FTA	fault tree analysis
HAEM	health-aware energy management
HBI	hierarchical Bayesian inference
LB	learning-based
MCR	maximum continuous rating
MOCP	multi-objective optimal control problems
MPC	model predictive control
OB	optimisation-based
PHM	proportional hazard model
PMP	Pontryagin's minimisation principle
PTI	power take in
PTO	power take out
RB	rule-based
RCM	reliability centred maintenance
RL	reinforcement learning
RUL	remaining useful life
STPA	system theoretic process analysis
WPHM	Weibull proportional hazard model

degradation and prolong system lifetime expectancy [19].

The existing literature reports several methods to tackle the energy management of hybrid power plants. These are mainly categorised into the following three types: rule-based (RB), optimisation-based (OB), and learning-based (LB) [20]. The most widely used In the maritime sector include dynamic programming (DP) [21], Pontryagin's minimisation principle (PMP) [22], equivalent consumption minimisation strategy (ECMS) [23], model predictive control (MPC) [24], and Reinforcement Learning (RL) [25,26].

Frequently, the energy management strategies for marine applications focus mainly on fuel savings and emissions reduction. Recent studies [23,27] demonstrated the ECMS to ship hybrid propulsion systems achieving considerable fuel savings compared to rule-based approaches. The MPC method using the receding horizon prediction technique also exhibited considerable fuel consumption reduction in hybrid marine propulsion systems [24,28]. Wu et al. [25] applied a double Q reinforcement learning method to a hybrid fuel cell and battery propulsion system, achieving close to optimal results in different operating profiles. Planakis et al. [29] proposed an MPC framework employing a trade-off strategy between fuel consumption and NOx emissions minimisation. Taheri et al. [30] formulated an optimisation method for the operation of a power system considering fuel consumption and CO_2 emissions reduction. Nevertheless, these methods do not consider how the power allocation at every instant affects the component health state or reliability, and consequently the system behaviour.

To assess the health state of ship power plants, the operating history, the prevailing environmental conditions and the plant operating conditions need to be considered. Advanced monitoring capabilities are needed for diagnosing the current health state as well as providing prognosis of the plant's future behaviour. BahooToroody et al. [31] proposed a machine learning approach in a hierarchical Bayesian inference framework (HBI) to calculate the remaining useful life (RUL) of an autonomous ship's main engine with different degrees of autonomy using actual measurements. Abaei et al. [6,32] utilised probabilistic models using the Bayesian inference to calculate reliability metrics for unattended power plants considering unexpected and disruptive events. Bolbot et al. [33] proposed a monitoring methodology for cruise ship power plants, using sensor measurements to predict the dynamic blackout probability. Eriksen et al. [34] examined the applicability of a Reliability Centred Maintenance (RCM) method to assess maintenance and reliability in an unmanned vessel. Lee et al. [35] used fault tree analysis (FTA) as a risk tool to support risk-informed decision-making for an autonomous collision avoidance system.

System-level monitoring methods are required to assess the ship power plant's health state, which depends on the system layout, components and their interconnections. Dynamic Bayesian networks (DBN) constitute an emerging method for predicting a complex system's health state [36], capturing the temporal dependencies between the modelled components [37]. Guo et al. [38] presented an approach based on a DBN to evaluate the operational reliability of a marine propulsion system by combining both monitoring and statistical data. Rebello et al. [39] used DBN to integrate components' degradation state into the system's functional state. Gao et al. [40] utilised a DBN to evaluate the reliability of an unmanned surface vehicle, by capturing the interactions at the component and subsystem levels.

Nonetheless, the combination of energy management strategies and monitoring methods for reliability and health assessment has not been

widely used in the marine industry. Tang et al. [18] used a static optimisation method for the energy management of a hybrid ship power plant employing models to predict the battery RUL, aiming to minimise emissions and fuel consumption whilst extending the battery's lifetime. Hein et al. [41] applied a multi-objective optimisation method for the energy management of a hybrid ferry considering battery degradation. Johansen and Utne [42,43] integrated System theoretic process analysis (STPA) and Bayesian networks to enable supervisory risk control for autonomous ships. For autonomous ship power plants, the integration of health assessment and the energy management strategy can be employed to develop the enabling technology for intelligent decision-making to provide the necessary resilience in the case of unexpected failure events and maximise the plant reliability [44].

The concept of health-aware control combining control strategies with health monitoring methods was proposed by Escobet et al. [45] to address the challenge of health monitoring and management for complex systems, demonstrating its application to a conveyor belt system. Salazar et al. [46] applied the same concept to a drinking water network considering the trade-off between control performance and system reliability. Pour et al. [47] included the health-aware aspect for the control of water networks using system reliability in the objective function. Balaban et al. [48] proposed an approach to unify prognostics and health management with automated decision-making for complex systems in the presence of uncertainties. Based on these studies' findings, it is anticipated that the health-aware control concept can benefit the development of maritime autonomous and intelligent systems, hence, it is investigated herein.

From the preceding literature review, the following research gaps are revealed: (a) employed energy management studies for hybrid power plants focus mainly on the minimisation of performance metrics to achieve fuel savings and emissions reduction; (b) the ship power plant health metrics like reliability and risk are not integrated into the energy management strategies; (c) only a few studies have demonstrated decision-making capabilities combining health and reliability monitoring with performance criteria.

This study aims to develop a health-aware energy management (HAEM) approach that integrates the health monitoring information from reliability tools with energy management. The system reliability is calculated and used as the health metric targeting to avoid operating regions that can decrease both component(s) and system reliability. The proposed approach is applied to the case study of a pilot boat hybrid power plant.

To the best of the authors' knowledge, it is the first time that such an approach is presented in the pertinent literature. Additional novel contributions of this study include the investigation of the trade-off between fuel consumption and system reliability as well as the use of decision-making methods to determine the components' operating conditions.

The remainder of this study is structured as follows. Section 2 describes the employed methodology along with the considered methods and models. In Section 3, the system description and the required input for the examined case study are presented. Section 4 presents and discusses the derived results. In Section 5, the main findings and conclusions of this study are summarised.

2. Developed health-aware energy management decision-making approach

2.1. Overview

The proposed HAEM approach consists of the following modules: (a) the hybrid power plant model; (b) the decision-making based on the utopian point method; (c) the energy management system; (d) the dynamic reliability estimator with the failure update model. Fig. 1 presents the block diagram of the HAEM which highlights the main tools/modules employed and their interactions in the closed loop system, as well as the key input/output parameters. The HAEM approach is applied to a ship hybrid power plant that includes an engine, an induction machine and a battery as the energy storage system.

The hybrid power plant model is developed by combing physical and surrogate sub-models to sufficiently represent the physical system performance. The energy management is based on ECMS, which is capable to handle unknown operating profiles by converting the problem of minimising fuel consumption into an instantaneous optimisation problem, thus achieving near-optimal fuel savings [23].

A DBN approach is adopted to estimate the dynamic variation of the considered system reliability. A Weibull proportional hazard model (WPHM) model is employed to consider the dependence of the failure rate on the components' operating points. In addition, to capture the time-dependency for the component reliability estimation, a semi-Markovian approach is adopted, which can implicitly update the component reliability based on the elapsed time.

At every instance of the power-split problem, an optimal fuel consumption point is identified by the energy management strategy, whereas an optimal system reliability point is proposed by the DBN. The Pareto front is developed with these two objectives, and the reference or utopia point method is used to identify the plant components' operating points based on the distance minimisation to an infeasible target [49,50].

2.2. Hybrid power plant model

Energy management strategies require the assessment of several operating points at every timestep. In these cases, high-fidelity models can significantly increase the modelling complexity and computational cost [51]. On the contrary, quasi-static modelling approaches are sufficient to calculate the fuel consumption and the power plant components' performance parameters [52]. As a result, the investigated power plant components are modelled by employing efficiency maps, fuel consumption maps and first principles models.

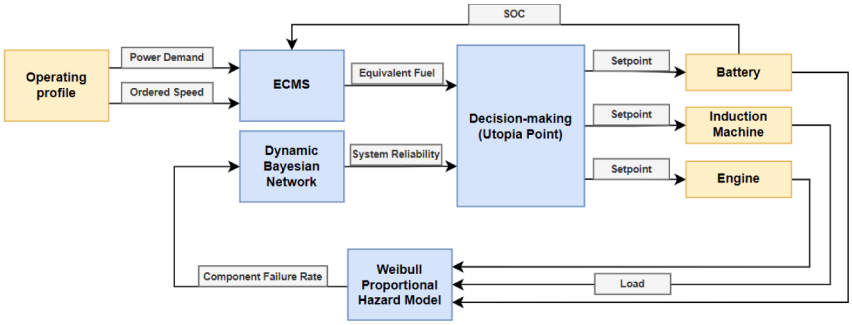

Fig. 1. Block diagram of the HAEM approach.

2.2.1. Marine engine model

The brake-specific fuel consumption (BSFC) of marine engines depends on the operating point (brake power and rotational speed). This study employs the BSFC map, which is developed by employing the engine manufacturer data, to calculate the engine fuel mass flow rate as a function of engine speed and torque [52]:

$$\dot{m}_f = f_{eng}\left(Q_{eng}, N_{eng}\right) \tag{1}$$

where $\dot{m}_f$ is fuel flow mass rate, Q_{eng} is the engine torque and N_{eng} is the engine rotational speed.

2.2. Electric machine model

To calculate the mechanical power and the mechanical losses of the electric machine an approach based on its efficiency map is used [53]. and the load correction factor is employed [54]. The provided mechanical power P_{em} is expressed as:

$$P_{em} = \eta_{em}(P_{elec}) N_{em} Q_{em}, \quad P_{elec} \geq 0 \ (Motoring\ Mode) \tag{2}$$

$$P_{em} = \frac{1}{\eta_{em}(P_{elec})} N_{em} Q_{em}, \quad P_{elec} < 0 \ (Generating\ Mode) \tag{3}$$

where η_{em} denotes the electric machine efficiency, Q_{em} denotes the electric machine torque, P_{elec} denotes the machine's electrical power, and N_{em} denotes the electric machine rotational speed.

2.2.3. Battery model

The battery performance is modelled by employing the quasi-static approach considering the first-order equivalent circuit [52]. The current I is calculated as a function of power using the following formula:

$$I = \frac{V_{oc}}{2R_0} - \sqrt{\left(\frac{V_{oc}}{2R_0}\right)^2 - \frac{P_{bat}}{R_0}} \tag{4}$$

where P_{bat} is the battery power, V_{oc} is the open circuit voltage, R_0 is the series resistance.

The battery state of charge (SOC) time variation in the next timestep is calculated as:

$$SOC(t+\Delta t) = SOC(t) - \frac{V_{oc} - \sqrt{V_{oc}^2 - 4P_{bat}R_0}}{2Q_{max}R_0} \tag{5}$$

where Q_{max} is the battery capacity.

It should be noted that this model does not consider the ageing effects of the battery due to the loading cycles, whereas the influence of the battery temperature is also considered negligible [55].

2.2.4. Propeller load

To model the absorbed power propeller, the propeller law is used [56]. Based on the engine maximum continuous rating (MCR) point, the propeller torque Q_{prop} is calculated by:

$$Q_{prop} = k_p N_{eng}^2 \tag{6}$$

where the k_p coefficient is calculated at the MCR point.

2.3. Energy management strategy (ECMS)

2.3.1. Overview

The ECMS converts the global optimisation problem of finding the minimum fuel consumption to an instantaneous optimisation problem based on arguments for the energy flow in the power plant whilst satisfying various constraints [52]. This attribute enables its real-world implementation, as energy management is formulated as an optimisation problem to be solved at every instant, considering the requested power setpoint.

The conversion to the instantaneous problem is performed using an equivalence factor, which is tuned for a typical operating profile. Nevertheless, it has been shown that ECMS can achieve significant robustness in different operating profiles whilst finding near-optimal solutions [23]. Furthermore, the ECMS does not require information about the future operating profile, compared to receding horizon techniques, thus is can significantly mitigate the computational burden [27].

2.3.2. Optimisation problem formulation

The underlying idea behind ECMS is that a cost is assigned to the electrical energy to render it equivalent to the amount of fuel that can be saved or consumed. As a result, the instantaneous equivalent fuel mass flow rate $\dot{m}_{f,eqv}(t)$ is the sum of the engine fuel mass flow rate and the equivalent or virtual fuel mass flow rate corresponding to the rechargeable energy storage system $\dot{m}_{ress}(t)$:

$$\dot{m}_{f,eqv}(t) = \dot{m}_f(t) + \dot{m}_{ress}(t) \tag{7}$$

The equivalent or virtual fuel mass flow rate is calculated using an equivalence factor, which is estimated using a typical operating profile. Usually, the equivalence factor varies for the charging and discharging phases respectively [52]. Nevertheless, a single value suffices to capture the efficiency in the electrical path [23]. Consequently, the equivalent or virtual fuel flow mass rate is calculated by:

$$\dot{m}_{ress}(t) = s(t)\frac{P_{bat}}{Q_{LHV}} \tag{8}$$

where $s(t)$ is the equivalence factor and Q_{LHV} is the fuel's lower heating value at ISO conditions (corresponding to 42,700 kJ/kg according to ISO 3046 [57]).

To guarantee that the SOC does not exceed the admissible limits, a penalty function is introduced [52]. The penalty function adjusts its value based on the deviation of the SOC from its target value SOC_t ($p(SOC) < 1$ for $SOC > SOC_t$, resulting in a lower cost attributed to battery energy, increasing the discharge likelihood, whereas $p(SOC) > 1$ when $SOC < SOC_t$, increasing the cost of battery energy and reducing the discharge likelihood). The penalty function takes the following form:

$$p(SOC) = 1 - \left(\frac{SOC(t) - SOC_t}{(SOC_{max} - SOC_{min})/2}\right)^3 \tag{9}$$

The equivalent or virtual fuel flow mass rate is then calculated according to the following equation:

$$\dot{m}_{ress}(t) = s(t)\frac{P_{bat}}{Q_{LHV}} p(SOC) \tag{10}$$

The control variable u denotes the provided power by the battery P_{bat}, whereas the exogenous input parameters include the battery SOC, the requested propulsive power P_{prop}, and the propeller rotational speed N_{prop}. The instantaneous equivalent fuel mass flow rate is subsequently calculated for several discrete candidate control variables. Finally, the optimal solution consists of the control parameters values to minimise the instantaneous equivalent fuel mass flow rate according to the following equation:

$$u^*(t) = \underset{u}{\operatorname{argmin}} \dot{m}_{f,eqv}\left(u, SOC, P_{prop}, N_{prop}\right) \tag{11}$$

The solutions must also satisfy various constraints for the provided power and the rotational speed of the electric machine and the engine whilst ensuring that the SOC does not exceed the permissible limits.

2.4. System reliability estimator

2.4.1. Dynamic Bayesian network (DBN)

A DBN is employed to calculate the system reliability based on the logical structure of the system, whilst considering the temporal dependencies to predict the liability in future time steps [38]. The

components and system reliability is employed herein to represent the system health state, as reliability expresses the probability of a component performing the required function at a specific time period [17,46,47].

The DBN is an extension of the Bayesian network (BN), which captures network the temporal behaviour [58]. Bayesian networks are probabilistic directed acyclic graphs, which employ nodes to represent variables and edges to characterise the dependencies between these variables whilst using conditional probabilities tables (CPT) to quantify these dependencies. The nodes and edges constitute the qualitative part of the BN, whilst the conditional probabilities enable the quantitative analysis. The joint probability distribution in the Bayesian network is given by the following equation [59]:

$$P(X_1, X_2, \ \ldots, X_n) = \prod_{i=1}^{n} P(X_i | Pa(X_i)) \tag{12}$$

where $Pa(X_i)$ represents the parent set of any variable X_i, and $P(X_i|Pa(X_i))$ is the conditional probability distribution function of variable X_i given its parent set.

Unlike BNs which are static models, DBNs can represent several time slices, where the nodes between the different time slices can be connected with directed temporal edges to unveil the temporal dependencies. The transition between the previous time slice and the current time slice is expressed by the following equation [59]:

$$P(Z_t | Z_{t-1}) = \prod_{i=1}^{n} P\left(Z_{i,t} \middle| Pa\left(Z_{i,t}\right)\right) \tag{13}$$

where Z is the family of random variables X_1,X_2, to X_N, $Z_{i,t}$ is the ith node at the time slice t, and $Pa(Z_{i,t})$ is the parent nodes of $Z_{i,t}$ from the same and previous time slices.

Consequently, the final joint probability distribution for all the time slices takes the following form [59]:

$$P(Z_{1:N}) = \prod_{t=1}^{N} \prod_{i=1}^{n} P\left(Z_{i,t} \middle| Pa\left(Z_{i,t}\right)\right) \tag{14}$$

Since the DBN in this study is used to calculate the overall system reliability, the approach proposed by Bobbio et al. [60] is followed, where fault trees are mapped into Bayesian networks. Firstly, the components of the power plants are modelled as root nodes with the component reliability being provided as input, which gets updated at every timestep. The next step is to model the interconnections between the component nodes to capture their effect on the subsequent system behaviour. As a result, intermediate nodes are used, which represent the causal relationships equivalent to logical gates found in fault trees (AND/OR gates). These nodes are modelled as noisy gates by specifying accordingly the CPT tables [61].

To carry out the quantitative analysis, the calculations are performed using the SMILE engine, which is developed in C++ [62]. Since the modelling has been implemented in the MATLAB environment, a wrapper was used to import the SMILE engine into MATLAB. This toolbox supports the use of virtual evidence as input [63], where the evidence is provided in the form of a probability distribution.

Furthermore, the DBN employs two time slices for which the DBN input parameters are updated at each timestep. The first time slice estimates system reliability at the current time step, whereas the second time slice calculates system reliability at the end of the considered timestep, considering the influence of the components' operating points. The forecasted system reliability in the various investigated operating points is used as input for the decision-making method discussed in the following sections.

2.4.2. Components reliability

The constituent parts of the DBN that get updated at every timestep are the root nodes, which represent the random variables pertinent to the components' reliability. As reliability is a function that depends on time, the components' reliability must be calculated at every timestep of the energy management strategy and update the root nodes of the DBN.

Furthermore, the operating point of each power plant component influences both the performance and the component reliability, consequently the remaining component lifespan [18]. As a result, it is needed to capture the influence of the operating point on each component reliability, whilst considering the effect of the previous operational history.

In this respect, a WPHM is used to update the failure rate in each time step to account for the influence of the operating point variation. The WPHM is an extension of the classical proportional hazard model (PHM) introduced by Cox [64], where the failure rate function follows the Weibull distribution [65]. Contrary to exponential approaches where the failure rate is constant, using values of the Weibull distribution shape factor (β) greater than 1 results in increasing the failure rates with time; thus, capturing the components' reliability decrease. According to the WPHM, the failure rate $\lambda(t,l)$ is given by [49]:

$$\lambda(t,l) = \beta \lambda_0^{\beta} t^{\beta-1} g(l,\theta) \tag{15}$$

where λ_0 is the baseline failure rate, whereas the function g(l,θ) is called the covariate function that depends on the covariate l representing the component load and a component parameter θ.

In health-aware control applications, the covariate function of the load can take many forms including exponential, linear and quadratic [17,46]. In this study, the linear form is chosen where the values for the failure rates are based on the OREDA database [66]. In particular, the mean and maximum values of the failure rate (λ_{mean} and λ_{max}) are considered, whereas the failure rate is considered a linear function of the load [67]. The component failure rate is thus expressed according to the following equation:

$$\lambda(t,l) = \beta \lambda_{mean}^{\beta} t^{\beta-1} \left(1 + \left(\left(\frac{\lambda_{max}}{\lambda_{mean}}\right)^{\beta} - 1\right) l\right) \tag{16}$$

where l is the specific power plant component load.

This model is used for all the components except for the engine, where its failure rate is modelled to depend also on the engine speed. More specifically, regions of the engine operating envelope close to the torque/speed limit as well as low loads are preferred to be avoided, as they can potentially accelerate degradation. Thus, it is assumed that the engine failure rate exhibits its maximum values for loads of 20% (and less) and at the torque limit region. For the other operating regions, the engine failure rate is a linear function of the load. According to the considered WPHM, the engine failure rate is calculated by the following equations:

$$\lambda(t,l) = \beta \lambda_{max}^{\beta} t^{\beta-1}, \quad 0 \le l < 0.2 \tag{17}$$

$$\lambda(t,l) = \beta \lambda_{mean}^{\beta} t^{\beta-1} \left(1 + \left(\left(\frac{\lambda_{max}}{\lambda_{mean}}\right)^{\beta} - 1\right) \frac{l - 0.2}{l_{limit} - 0.2}\right), \ 0.2 \le l < 1 \tag{18}$$

where l_{limit} the maximum load at every engine speed at the torque/speed limit curve.

Since the values of the failure rates from the OREDA database are considered constant, a transformation is necessary for their use in the Weibull distribution. The correction procedure as described by Denson et al. [68] is followed herein.

The power plant components' failure rates are calculated at every timestep using Eqs. (16)–(18). For operational components in the current time step, these failure rates provide information to calculate the conditional probability of the component failing in the next time step. Nonetheless, it is essential to calculate the system and components' reliability time variation by including the influence of the previous operating points and the past operational time. In this respect, a

nonhomogeneous semi-Markov chain is adopted.

In the classical Markov chain, the future states depend only on the present state without considering history (memoryless property) [69]. By extending the Markov chain to a semi-Markov chain, a stochastic process can be modelled where transitions can occur at different times, satisfying the Markov property of each transition [70]. The difference between a homogeneous semi-Markov chain and a nonhomogeneous semi-Markov chain is that in the former transition probabilities are independent of time, whereas in the latter they depend on the current state and the elapsed time.

In this respect, a nonhomogeneous semi-Markov chain is built for every component with a discrete random variable x_i having two mutually exclusive states (working or failure) and the transition probabilities matrix [46] according to the following equation:

$$P(x_i(k+1)|x_i(k)) = \begin{bmatrix} 1-p_i(k) & p_i(k) \\ 0 & 1 \end{bmatrix} \tag{19}$$

where k denotes the current timestep, and $p_i(k)$ is the probability of the ith component failing in the next timestep $(k+1)$ given that it was working in the current timestep.

From the above definition, the probability $p_i(k)$ is calculated based on the failure rate definition [11] according to the following equation:

$$p_i(k) = \lambda_i(k,l)\Delta t \tag{20}$$

where Δt is the interval between the following and the current timestep.

Moreover, component reliability R_i is defined based on the failure rate using the following formula:

$$R_i(t) = e^{-\int_0^t \lambda_i(t,l)dt} \tag{21}$$

By discretising the above expression for the different timesteps, each component reliability is calculated as:

$$R_i(k) = e^{-T_s \sum_{k=0}^{k} \lambda_i(k,l)} \tag{22}$$

where T_s is the sampling interval of the timesteps.

Each component reliability is calculated for the next timestep based on the dictated operating profile, and subsequently, it is fed into the root nodes for the current and the next time slices of the DBN. The DBN gets updated at every execution of the energy management strategy by providing the components reliability of the next timesteps. It should be noted that the input of the root nodes is in the form of a probability distribution, as it represents reliability, which is provided to the DBN in the form of virtual evidence [39].

By using the WPHM and the semi-Markov chain, the past operational period and the influence of the previous points can be explicitly captured in the reliability of the components, whilst updating the components' reliability as evidence for the DBN to calculate the system reliability. Furthermore, the overall system reliability is calculated for every different operating point that satisfies the constraints dictated by the energy management strategy.

2.5. Decision-making method

In the previous sections, the calculations of the instantaneous equivalent fuel flow mass rate and the system reliability were presented. However, a single operating point should be identified for every power plant component. As indicated by the results presented in the next section, optimal fuel consumption and optimal system reliability do not always occur at the same operating point, as a result, a trade-off strategy should be followed to choose the operating point as a compromise between these two objectives.

The most straightforward approach to solving multi-objective optimal control problems (MOCP) is by a scalarisation technique using weighting factors [50]. A weighting factor is assigned to every objective, as a result, the control problem employs a single objective function that must be minimised or maximised. The weighting factors are typically determined by using experts' knowledge, which is not always available in the case of hybrid systems and autonomous operations. Consequently, a more sophisticated method should be followed, where the weight for each objective dynamically changes based on the power demand and the prevailing conditions.

This study employs, the reference or utopia point method [50,49], for facilitating decision-making. To select the components operating point at each time step, the Pareto front of the two selected objectives is identified. All the solutions in the Pareto front are feasible, however, the final solution is selected based on the distance minimisation to an infeasible target or utopia point. The distance to an infeasible target point T should be minimised, so that does not belong to the Pareto front J, according to the following equation:

$$\min_u \bar{J}(u) = \min_u T - J(u) \tag{23}$$

The infeasible point is identified as the point with the lowest equivalent fuel mass flow rate and the highest system reliability, which apparently cannot be achieved. Both objectives are scalarised from zero to unity based on their extreme values to make their contribution equal (their maximum values and minimum values are set to one and zero, respectively). An example of applying this method to the Pareto front of this case study is shown in Fig. 2. The circle at the bottom right corner represents the utopia point, while the other circle denotes the selected setpoint which is selected based on the calculated minimum distance highlighted by the dashed line. This process of building the Pareto front and minimising the distance to the utopia point is repeated in every time step.

3. Case study description

The HAEM approach is demonstrated in the case study of a parallel hybrid power plant of a pilot boat. A schematic representation of the investigated power plant configuration is presented in Fig. 3.

This study models the mechanical and electrical components of the considered power plant. For operating autonomously, additional components are expected pertinent to software, sensors, actuators, intelligent monitoring and communications. However, these are considered out of this study's scope.

3.1. Operating profile

To examine the behaviour of the HAEM approach as close as possible to real operating conditions, available engine speed data corresponding

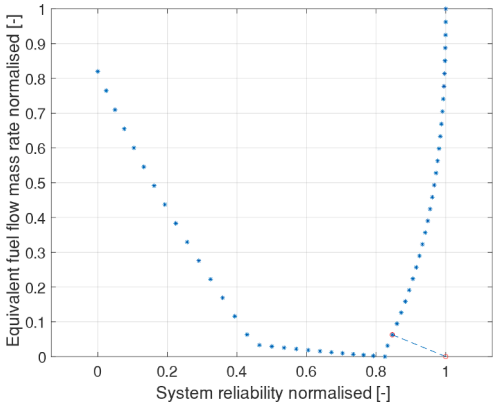

Fig. 2. Example at a specific timestep of the Pareto front with the two objectives normalised.

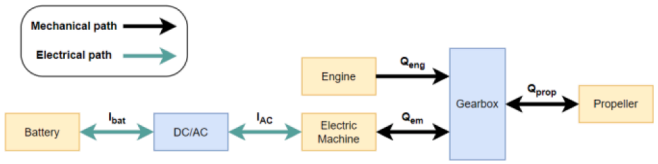

Fig. 3. Parallel hybrid power plant configuration.

to three voyages, which were acquired from a pilot boat equipped with a mechanical propulsion system and marine diesel engines, were employed.

Subsequently, the demanded propulsion power that is required as input is estimated by using the propeller law, i.e., considering the cubic function of the provided engine speed. Furthermore, the recorded speed has an inherent noise due to the operating condition disturbances and the sensor's uncertainty, thus filtering was performed to provide the power setpoints. Fig. 4 presents the power setpoints combining the three sample voyages.

Based on the power demand profile for these voyages, a half-month operating profile was developed by arranging the three voyages in random order as well as by altering the power setpoints with $a \pm 10\%$ random variation to represent a more realistic scenario.

3.2. Models input

The characteristics of the selected power plant components are presented in Table 1. The hybrid configuration is of the parallel type, which indicates that the two prime movers (diesel engine and the electric machine) are coupled in a gearbox providing power either individually or simultaneously to the propeller. In the power take in (PTI) mode, the electric machine operates as a motor receiving energy from the battery and providing power to the propeller. In the power take out (PTO) mode, the electric machine operates as a generator charging the battery.

The engine manufacturer data were employed to develop the fuel consumption map. In particular, the considered marine engine is the Scania DI16M, which is a twin-turbo four-stroke diesel engine [71]. For the other components, the models described in Section 2 were deployed with the system parameters provided in Table 1. All the models were implemented in the MATLAB environment Table 2.

3.3. Reliability models input

The developed DBN has a qualitative and a quantitative part. The qualitative part presents the structure of the network showing the nodes' interconnections. Fig. 5 presents the developed DBN for the investigated ship hybrid power plant, where the arcs above the root nodes represent the temporal dependences.

Table 1
Investigated hybrid power plant parameters.

Component	Parameter	Value
Engine	Type	4 stroke, 8 cylinders
	Power MCR (kW)	423
	Speed MCR (RPM)	2100
Electric Machine	Nominal power (kW)	100
Battery	Type	Lithium-ion
	Module capacity (Ah)	100
	Nominal Voltage (V)	12
	Number of modules	100

Table 2
Failure rates and shape parameters for the considered components.

Component	Maximum failure rate (h^{-1})	Mean failure rate (h^{-1})	Shape parameter β (–)
Engine	$32.42\ 10^{-4}$	$17.68\ 10^{-6}$	2.4
Electric Machine	$97.56\ 10^{-6}$	$43.76\ 10^{-6}$	1.2
Battery	$136.81\ 10^{-6}$	$63.57\ 10^{-6}$	1.69
Gearbox	$3.80\ 10^{-6}$	$1.01\ 10^{-6}$	2.028

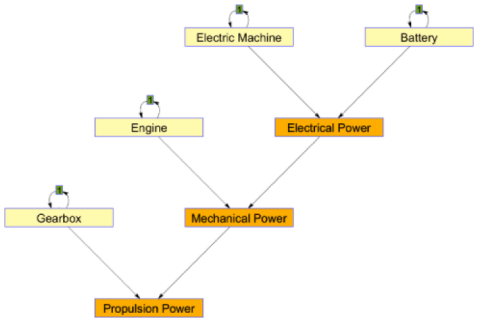

Fig. 5. Unrolled dynamic Bayesian network structure.

The components' reliability is calculated in every timestep and is used as an input in the form of virtual temporal evidence to the DBN. In addition, for the intermediate nodes, noisy-OR gates were used to speed up the inference computation [63].

Furthermore, the values for the shape parameters employed for the WPHM are based on the data reported in [67]. The failure rates are taken from the OREDA database, whereas their mean and maximum values are chosen by aggregating all the failure modes of the investigated components.

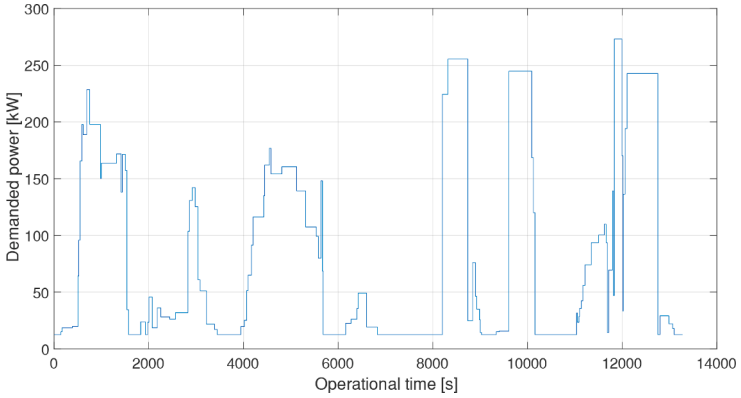

Fig. 4. Sample operating profile with the three sample voyages combined.

4. Results and discussion

4.1. Energy management strategy evaluation

The use of the ECMS for energy management does not guarantee the globally optimal solution, as the problem is converted to an instantaneous minimisation problem for real-world applications, where the operating profile is not known a priori. However, it can achieve near-optimal solutions with a considerably low computational burden.

Furthermore, the results obtained are greatly affected by the selection of the equivalence factor [23]. In this study, the equivalence factor is considered constant and is tuned based on the employed operating profile. The selection of the equivalence is based on the shooting method as described in [52].

Moreover, to verify ECMS, a comparison was made with Dynamic Programming (DP). In the energy management problem of hybrid configurations, DP is the method that approximates the globally optimal solution, since the full history of the operating profile is provided as input and the optimisation problem is solved backwards in time [72].

This study employs the DP function developed in [73]. The state variable (SOC) is discretised considering Nx=101, whereas the control variables were discretised with Nu=201 values. To make the comparison equivalent the same discretisation was performed for the ECMS. In addition, the DP function enables the use of the boundary line, which provides more accurate results with fewer function evaluations [73].

Fig. 6 presents the time variations of the battery SOC and consumed fuel amount, which were derived by employing the DP and ECMS. The initial SOC is set to 70% for both methods. The total fuel consumption calculated by ECMS is 3.2% more than the global optimal solution achieved by the DP, demonstrating that ECMS is an effective strategy to achieve near-optimal results with a relatively low computational cost. However, there exists a slight difference in the final SOC value, which can be expected as in DP final state is explicitly set by the user, contrary to ECMS.

4.2. Half-month operating profile results

In this section, the results for the half-month operating profile are presented. It should be noted that the half-month operating profile refers only to the operational time and not the calendar time. Calendar time is longer, as the ship does not operate continuously. In addition, the initial reliability of the investigated components of the power plant is set to 0.95, to represent a close-to-new condition.

To reveal the advantages of the HAEM approach incorporating health-aware capabilities, a comparison is made against the ECMS considering the same operating profile. ECMS only employs the objective of reducing the total fuel consumption, consequently, it can be used as a benchmark to unveil the differences in the components and the hybrid power plant reliability as well as the total fuel consumption.

Since the power setpoints for the half-month operating profile are too many to be plotted in a single diagram, only the sample operating profile is presented in Fig. 7 to examine how the ECMS and HAEM dictate the setpoints for the investigated hybrid power plant components. In low loads where the engine exhibits high BSFC values, the electric machine operates using energy from the battery to provide the requested power to the propeller. In high loads where the engine exhibits lower BSFC values, the engine provides power for covering the propeller demand and charging the battery. This behaviour is spotted in both methods.

Fig. 8 presents a comparison of the battery SOC values along the half-month operation for both strategies. This study assumed that the initial battery SOC is 70% whereas the battery charging takes place via power generated from the diesel engine operation (shore/port stations charging was not considered). It can be inferred from Fig. 8 that in both strategies the battery SOC exhibits distinct cycles of discharging and charging. Nonetheless, both methods succeed in keeping the SOC around the set target value. The ECMS manages to keep the average value to the target of 70% through the implementation of the penalty function described in the previous section. However, the HAEM approach leads to the initial SOC decrease for the first 20 h operating period. This means that the battery provided more power/energy compared to the engine during this period, which is attributed to the battery's lower failure rate compared to the engine. However, it manages to keep the SOC target value to around 55% throughout the considered time period, avoiding the risk of keeping the battery at low SOC.

To quantify the fuel savings, Fig. 9 presents the total (cumulative) fuel consumption for the considered operating period derived from the two approaches as well as the fuel consumption of the baseline power plant. It is evident that the hybrid configuration with the ECMS results in a fuel reduction of around 17% compared to the baseline configuration (conventional power plant). This behaviour is in alignment with results from pertinent studies dealing with the potential reductions in fuel and operational cost [15,26].

Moreover, the HAEM approach resulted in an increase of the total fuel consumption by around 1.5% compared to the ECMS. This is attributed to the employed trade-off between fuel consumption and system reliability. As a result, the engine operates in higher reliability regions, at the expense of slightly increased fuel consumption.

Fig. 10 presents the comparison of the system reliability calculated in the terminal node for the ECMS and HAEM, respectively. To determine the system reliability time variation using HAEM, two time slices were considered at 150 and 300 h, respectively. The system reliability increases compared to the scenario where the ECMS is employed, by 0.015 at 150 h and 0.029 at 300 h. Since these values represent probabilities and cannot be interpreted explicitly, the failure rate was estimated by differentiating Eq. (21) at the same time slices. At 150 h the overall system failure rate is estimated to be 2.97 10^{-6} h^{-1} and 3.28 10^{-6} h^{-1} with the ECMS and HAEM, respectively. At 300 h, the overall system

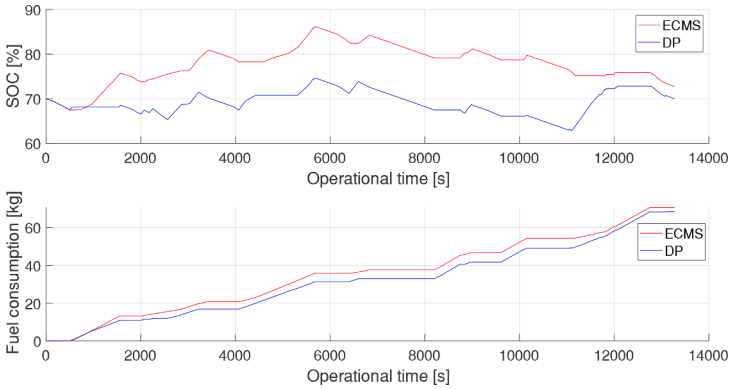

Fig. 6. Performance comparison of ECMS with DP.

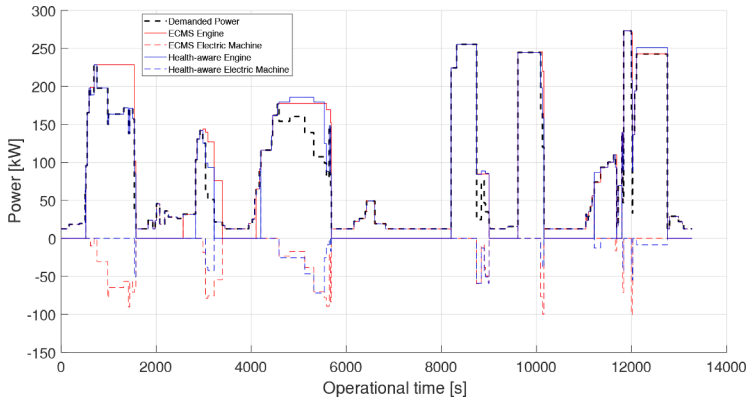

Fig. 7. Power plant components operating setpoints results.

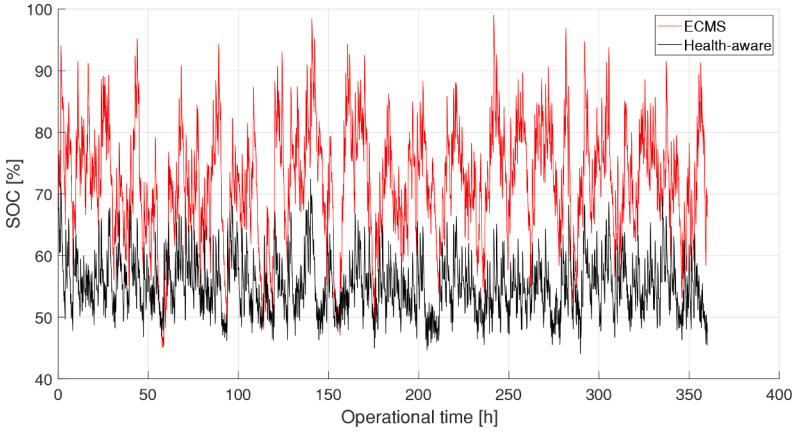

Fig. 8. Battery State of Charge results.

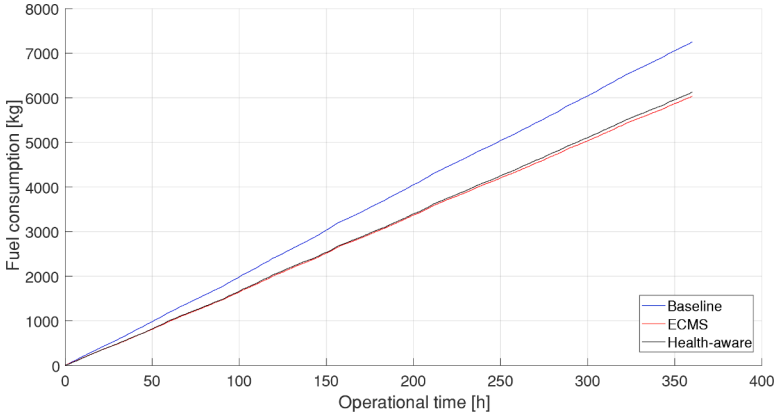

Fig. 9. Total (cumulative) fuel consumption comparison results.

failure rate is found 2 10^{-6} and 7.65 10^{-6} h^{-1} for the ECMS and HAEM, respectively, which is almost 4 times smaller compared to ECMS. Apparently, the HAEM gains are more evident as the operating period of the hybrid power plant increases, resulting in prolonging the system's lifetime expectancy as well as retaining high reliability, which is one of the crucial requirements for autonomous operations.

As the engine is the power plant component with the highest failure rate, it is considered the most critical for autonomous operations. Fig. 11 presents the engine reliability time variations for the two approaches and the baseline power plant. It is evident that when the engine only provides the required power (baseline configuration), its reliability decreases rapidly to unacceptable levels for autonomous operations. It is noted that the MUNIN project recommended that the engine should operate reliably without human intervention for 500 h [6]. It is also expected that maintenance activities during port calls will be performed for autonomous ships, which leads to retaining high reliability values.

Fig. 12 presents the engine load diagram with superimposed BSFC contours. The operating points derived from both the ECMS and HAEM are also shown in this figure. By using the proposed approach, operating points below 20% and near the torque limit are frequently avoided, thus resulting in engine prolonged lifetime and safer operation. On the contrary, the ECMS selects operating points in the whole operating region as

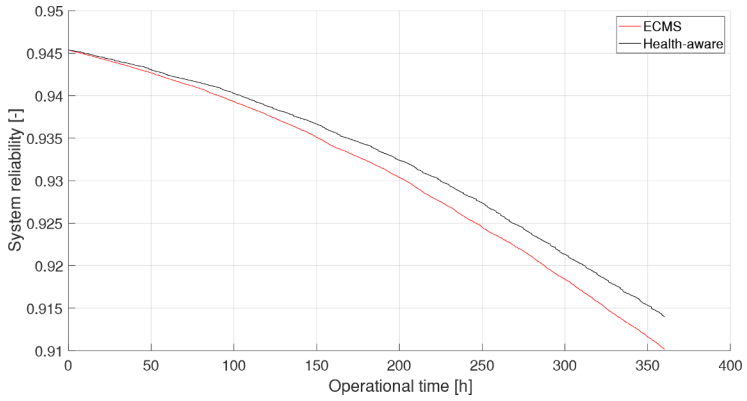

Fig. 10. Hybrid propulsion plant reliability time variation.

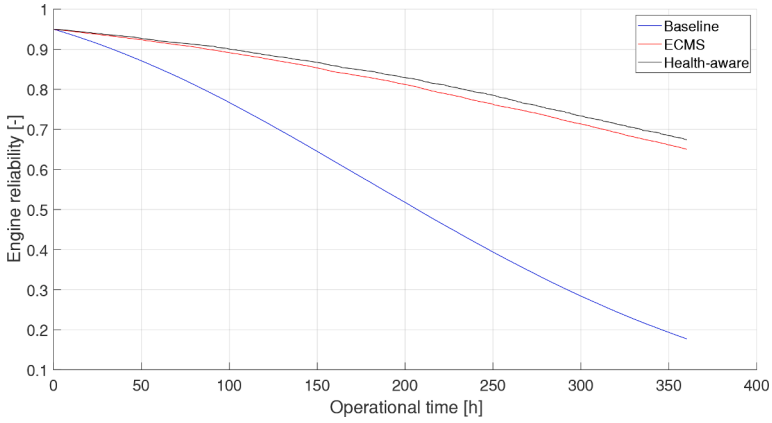

Fig. 11. Engine reliability evolution.

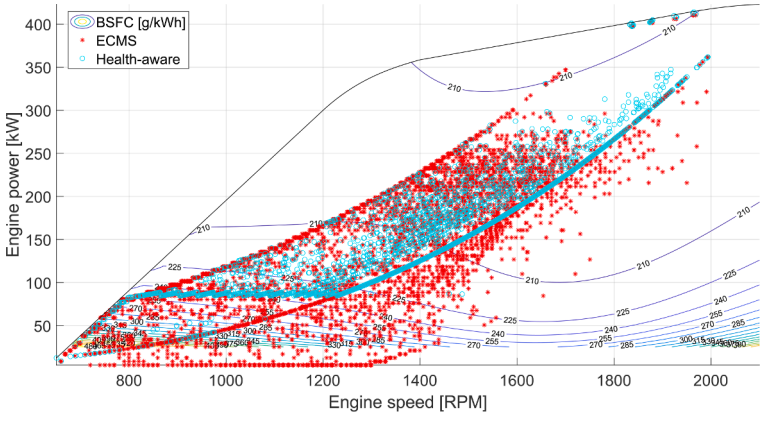

Fig. 12. Comparison of the engine operating points.

long the performance constraints are satisfied.

4.3. Discussion

The derived simulation results demonstrated the impact of the health-aware energy management decision-making (using the utopia method considering the contradictory objectives to minimise the fuel consumption and retain the plant reliability) on the considered hybrid power plant. The consideration of the health state by using reliability as the health indicator provides additional capabilities in decision-making. The proposed HAEM approach considers the influence of the component's operating conditions on their failure rate and effectively combines a reliability method and an energy management strategy. The DBN was used to calculate the dynamic reliability whilst revealing the interactions between the power plant components. Systems with multiple components of various types exhibit increased complexity and may involve unpredictable interactions, thus influencing system functionality in a complex manner [74].

The HAEM approach is based on decision-making that integrates the system health monitoring with the energy management. Thus, it can be effective for autonomous ship power plants, which due to the crew absence require extended monitoring and health assessment capabilities as well as resilience to failures [9,10]. However, apart from the power plant main and auxiliary components, other intelligent systems and

technologies need to be also considered.

Nonetheless, the HAEM approach exhibits some limitations. The ECMS considered a constant equivalence factor, which was tuned based on the employed operating profile. However, in real conditions with varying operating profiles, this approach cannot guarantee optimal fuel savings [52]. To tackle this limitation, adaptive methods with varying equivalence factors can be used by providing estimates of future power demands [23]. Another limitation is that the reliability is estimated based on failure rates provided by databases and models of low computational effort. As the involved uncertainties (aleatory and epistemic) may affect the decision-making process, it is essential to consider the uncertainties of data and models [75], by incorporating information from sensors measurements and updating the system health status based on real-time evidence [76].

This study did not consider battery ageing, as the main aim was to demonstrate the proposed HAEM approach. Physical or data-driven models in the pertinent literature to estimate the battery RUL [77,78], whereas temperature models can be employed to consider the effect of charge-discharge cycles [79].

Another aspect that affects health estimation is system complexity. In this case study, the investigated power plant had a simple structure. Real applications include complex topologies with interdependent systems, subsystems and components [80]. This case study did not consider the response to failure scenarios. For autonomous operations, the response to faults and failures must be investigated, as fault tolerance and resilience are vital [42]. Future studies could investigate more complex systems along with critical failure propagation, whilst considering the system reconfiguration.

5. Conclusions

This study proposed a decision-making approach for the health-aware energy management of ship power plants demonstrating its application for the case study of a pilot boat hybrid power plant, benchmarking the derived results against ECMS. The main findings of this study are summarised as follows.

The HAEM approach considers the trade-off operation between fuel consumption and system reliability. The results demonstrated that the hybrid configuration brings substantial fuel savings of around 17% compared to the baseline configuration that has mechanical propulsion powered by a diesel engine. In addition, a rapid decrease in engine reliability was observed in the baseline configuration compared to the hybrid plant.

The HAEM approach demonstrated higher reliability levels at the expense of a slight increase in fuel consumption by 1.5% compared to ECMS. The overall system failure rate was reduced almost 4 times at 300 h of operational time by employing the HAEM compared to ECMS. Hence, improved power plant reliability as well as prolonged system lifetime expectancy and reduction of maintenance costs can be achieved.

For the engine, which is the most critical component, operation in more reliable regions can be achieved, which is expected to result in enhanced safety levels, avoiding rapid degradation.

This study is an initial step towards autonomous power plant operations. Future studies could focus on extending the energy management strategy and the reliability estimation, considering more complex system representations, investigating the injection of faults and addressing uncertainties.

Funding

Parts of this study was carried out in the framework of the AUTOSHIP project (AUTOSHIP, 2021), which is funded by the European Union's Horizon 2020 research and innovation programme under agreement No 815,012.

CRediT authorship contribution statement

Charalampos Tsoumpris: Methodology, Writing – original draft, Writing – review & editing, Software, Supervision, Funding acquisition. **Gerasimos Theotokatos:** Methodology, Writing – original draft, Writing – review & editing, Software, Supervision, Funding acquisition.

Declaration of Competing Interest

The authors declare no conflict of interest.

Data availability

Data will be made available on request.

Acknowledgment

The authors greatly acknowledge the funding from DNV AS and RCCL for the Maritime Safety Research Centre (MSRC) establishment and operation. The opinions expressed herein are those of the authors and should not be construed to reflect the views of EU, DNV AS and RCCL.

References

[1] de Vos J, Hekkenberg RG, Valdez Banda OA. The impact of autonomous ships on safety at sea – a statistical analysis. Reliab Eng Syst Saf 2021;210:107558. https://doi.org/10.1016/j.ress.2021.107558. February.
[2] Ramos MA, Thieme CA, Utne IB, Mosleh A. Human-system concurrent task analysis for maritime autonomous surface ship operation and safety. Reliab Eng Syst Saf 2019;195:106697. https://doi.org/10.1016/j.ress.2019.106697. MayMar. 2020.
[3] Heffner K, Rødseth EJ. Enabling technologies for maritime autonomous surface ships. J Phys Conf Ser 2019;1357(1). https://doi.org/10.1088/1742-6596/1357/1/012021.
[4] Bahootoroody A, Mahdi M, Valdez O, Montewka J. On reliability assessment of ship machinery system in different autonomy degree ; a Bayesian-based approach. Ocean Eng 2022;254:111252. https://doi.org/10.1016/j.oceaneng.2022.111252. March.
[5] Kooij C, Kana AA, Hekkenberg RG. A task-based analysis of the economic viability of low-manned and unmanned cargo ship concepts. Ocean Eng 2021;242:110111. https://doi.org/10.1016/j.oceaneng.2021.110111. May.
[6] Abaei MM, Hekkenberg R, BahooToroody A. A multinomial process tree for reliability assessment of machinery in autonomous ships. Reliab Eng Syst Saf 2021;210:107484. https://doi.org/10.1016/j.ress.2021.107484. JanuaryJun.
[7] Chang CH, Kontovas C, Yu Q, Yang Z. Risk assessment of the operations of maritime autonomous surface ships. Reliab Eng Syst Saf 2021;207:107324. https://doi.org/10.1016/j.ress.2020.107324. September 2020.
[8] Wennersberg LAL, Nordahl H, Rodseth OJ, Fjortoft K, Holte EA. A framework for description of autonomous ship systems and operations. IOP Conf Ser Mater Sci Eng 2020;929(1). https://doi.org/10.1088/1757-899X/929/1/012004.
[9] Zio E. The future of risk assessment. Reliab Eng Syst Saf 2018;177:176–90. https://doi.org/10.1016/j.ress.2018.04.020. April.
[10] Edge W, Field C, Walsh K. The autonomous machinery design of Tx ship. International Naval Engineering Conference and Exhibition (iNEC 2020) 2020. https://doi.org/10.24868/issn.2515-818X.2020.026.
[11] Rausand M, Høyland A. *System Reliability Theory : Models, Statistical Methods, and Applications*. In: Series in Probability and Statistics. Applied Probability and Statistics. 2nd ed. Hoboken, NJ: Wiley; 2004.
[12] Grotli, E.I., T.A. Reinen, K. Grythe, A.A. Transeth, M. Vagia, M. Bjerkeng, P. Rundtop, E. Svendsen, O.J. Redseth, and G. Eidnes. ''SEATONOMY''.*OCEANS 2015 - MTS/IEEE Washington*, 2015, 1-7.
[13] Dubey A, Santoso S. A two-level topology design framework for reliable shipboard power systems. Inventions 2016;1(3). https://doi.org/10.3390/inventions1030014.
[14] Chae CJ, Kim M, Kim HJ. A study on identification of development status of MASS technologies and directions of improvement. Appl. Sci. 2020. https://doi.org/10.3390/app10134564.
[15] Geertsma RD, Negenborn RR, Visser K, Hopman JJ. Design and control of hybrid power and propulsion systems for smart ships: a review of developments. Appl Energy 2017;194:30–54. https://doi.org/10.1016/j.apenergy.2017.02.060. Elsevier Ltd.
[16] Kim S, Choe S, Ko S, Sul S. Power system with a battery energy storage system. IEEE Electrif Mag 2015;3:22–33.
[17] Zagorowska M, Wu O, Ottewill JR, Reble M, Thornhill NF. A survey of models of degradation for control applications. Annu Rev Control 2020;50. https://doi.org/10.1016/j.arcontrol.2020.08.002.

[18] Tang W, Roman D, Dickie R, Robu V, Flynn D. Prognostics and health management for the optimization of marine hybrid energy systems. Energies 2020;13(18):4676. https://doi.org/10.3390/en13184676.

[19] Yue M, Jemei S, Zerhouni N. Health-conscious energy management for fuel cell hybrid electric vehicles based on prognostics-enabled decision-making. IEEE Trans Veh Technol 2019;68(12):11483–91. https://doi.org/10.1109/TVT.2019.2937130.

[20] Tran DD, Vafaeipour M, El Baghdadi M, Barrero R, Van Mierlo J, Hegazy O. Thorough state-of-the-art analysis of electric and hybrid vehicle powertrains: topologies and integrated energy management strategies. Renew Sustain Energy Rev 2020;119:109596. https://doi.org/10.1016/j.rser.2019.109596.

[21] Yuan Y, Chen M, Wang J, Yu W, Shen B. A novel hybrid energy management strategy of a diesel-electric hybrid ship based on dynamic programing and model predictive control. Proc Inst Mech Eng Part M J Eng Marit Environ 2022;236(3):644–57. https://doi.org/10.1177/14750902211068931.

[22] Zhang F, Wang L, Coskun S, Cui Y, Pang H. Computationally efficient energy management in hybrid electric vehicles based on approximate pontryagin's minimum principle. World Electr Veh J 2020;11(4):1–25. https://doi.org/10.3390/wevj11040065.

[23] Kalikatzarakis M, Geertsma RD, Boonen EJ, Visser K, Negenborn RR. Ship energy management for hybrid propulsion and power supply with shore charging. Control Eng Pract 2018;76:133–54. https://doi.org/10.1016/j.conengprac.2018.04.009. May.

[24] Antonopoulos S, Visser K, Kalikatzarakis M, Reppa V. MPC framework for the energy management of hybrid ships with an energy storage system. J Mar Sci Eng 2021;9(9):34–45. https://doi.org/10.3390/jmse9090993.

[25] Wu P, Partridge J, Bucknall R. Cost-effective reinforcement learning energy management for plug-in hybrid fuel cell and battery ships. Appl Energy 2020;275:115258. https://doi.org/10.1016/j.apenergy.2020.115258. May.

[26] Nuchturee C, Li T, Xia H. Energy efficiency of integrated electric propulsion for ships – a review. Renew Sustain Energy Rev 2020. https://doi.org/10.1016/j.rser.2020.110145.

[27] Xiang Y, Yang X. An ecms for multi-objective energy management strategy of parallel diesel electric hybrid ship based on ant colony optimization algorithm. Energies 2021;14(4):810. https://doi.org/10.3390/en14040810. Feb.

[28] Haseltalab A, Wani F, Negenborn RR. Multi-level model predictive control for all-electric ships with hybrid power generation. Int J Electr Power Energy Syst 2020;135:107484. https://doi.org/10.1016/j.ijepes.2021.107484. July2022.

[29] Planakis N, Papalambrou G, Kyrtatos N. Predictive power-split system of hybrid ship propulsion for energy management and emissions reduction. Control Eng Pract 2021;111:104795. https://doi.org/10.1016/j.conengprac.2021.104795. September 2020.

[30] Taheri SI, Vieira GGTT, Salles MBC, Avila SL. A trip-ahead strategy for optimal energy dispatch in ship power systems. Electr Power Syst Res 2021;192. https://doi.org/10.1016/j.epsr.2020.106917. May.

[31] BahooToroody A, Abaei MM, Banda OV, Kujala P, De Carlo F, Abbassi R. Prognostic health management of repairable ship systems through different autonomy degree; From current condition to fully autonomous ship. Reliab Eng Syst Saf 2022;221:108355. https://doi.org/10.1016/j.ress.2022.108355. August 2021.

[32] Abaei MM, Hekkenberg R, BahooToroody A, Banda OV, van Gelder P. A probabilistic model to evaluate the resilience of unattended machinery plants in autonomous ships. Reliab Eng Syst Saf 2022;219:108176. https://doi.org/10.1016/j.ress.2021.108176. April 2021.

[33] Bolbot V, Theotokatos G, Hamann R, Psarros G, Boulougouris E. Dynamic blackout probability monitoring system for cruise ship power plants. Energies 2021;14(20):6598. https://doi.org/10.3390/EN14206598. 202114, Page 6598Oct.

[34] Eriksen S, Utne IB, Lützen M. An RCM approach for assessing reliability challenges and maintenance needs of unmanned cargo ships. Reliab Eng Syst Saf 2021;210:107550. https://doi.org/10.1016/j.ress.2021.107550. FebruaryJun.

[35] Lee P, Theotokatos G, Boulougouris E, Bolbot V. Risk-informed collision avoidance system design for maritime autonomous surface ships. Ocean Eng 2023. Jan.

[36] Chemweno P, Pintelon L, Nganga P, Van Horenbeek A. Risk assessment methodologies in maintenance decision making : a review of dependability modelling approaches. Reliab Eng Syst Saf 2018;173:64–77. https://doi.org/10.1016/j.ress.2018.01.011. February.

[37] Jiang T, Zheng YX, Liu Y. Bayesian networks in reliability modeling and assessment of multi-state systems. Commun Comput Inf Sci 2019;1102:199–228. Springer Verlag.

[38] Guo Y, Wang H, Guo Y, Zhong M, Li Q, Gao C. System operational reliability evaluation based on dynamic Bayesian network and XGBoost. Reliab Eng Syst Saf 2022;225:108622. https://doi.org/10.1016/j.ress.2022.108622. May.

[39] Rebello S, Yu H, Ma L. An integrated approach for system functional reliability assessment using dynamic Bayesian network and hidden markov model. Reliab Eng Syst Saf 2018;180:124–35. https://doi.org/10.1016/j.ress.2018.07.002. Elsevier LtdDec. 01.

[40] Gao C, Guo Y, Zhong M, Liang X, Wang H, Yi H. Reliability analysis based on dynamic Bayesian networks: a case study of an unmanned surface vessel. Ocean Eng 2021;240. https://doi.org/10.1016/j.oceaneng.2021.109970. Nov.

[41] Hein K, Yan X, Wilson G. Multi-objective optimal scheduling of a hybrid ferry with shore-to-ship power supply considering energy storage degradation. Electron 2020;9(5). https://doi.org/10.3390/electronics9050849.

[42] Johansen T, Utne IB. Supervisory risk control of autonomous surface ships. Ocean Eng 2021;251:111045. https://doi.org/10.1016/j.oceaneng.2022.111045. August2022.

[43] Johansen T, Blindheim S, Torben TR, Utne B, Johansen TA, Sørensen AJ. Development and testing of a risk-based control system for autonomous ships. Reliab Eng Syst Saf 2023:109195. https://doi.org/10.1016/j.ress.2023.109195.

[44] Rødseth Ø.J., Faivre J., Hjørungnes S.R., Andersen P., Bolbot V., Pauwelyn A.S. and Wennersberg L.A.L. 2020 *AUTOSHIP deliverable D3.1: Autonomous ship design standards* Revision 1.0, June.

[45] Escobet T, Quevedo J, Puig V, Nejjari F. Combining health monitoring and control. Diagn. Progn. Eng. Syst. Methods Tech. 2012:230–55. https://doi.org/10.4018/978-1-4666-2095-7.ch012.

[46] Salazar JC, Weber P, Nejjari F, Sarrate R, Theilliol D. System reliability aware model predictive control framework. Reliab Eng Syst Saf 2017;167:663–72. https://doi.org/10.1016/j.ress.2017.04.012. May.

[47] Pour FK, Puig V, Cembrano G. Economic health-aware LPV-MPC based on system reliability assessment for water transport network †. Energies 2019;14(15):1–21. https://doi.org/10.3390/en12153015.

[48] Balaban E, Johnson SB, Kochenderfer MJ. Unifying system health management and automated decision making. J Artif Intell Res 2019;65:487–518. https://doi.org/10.1613/JAIR.1.11366.

[49] Gambier A. Multiobjective optimal control of wind turbines: a survey on methods and recommendations for the implementation. Energies 2022;15(2). https://doi.org/10.3390/en15020567.

[50] Peitz S, Dellnitz M. A survey of recent trends in multiobjective optimal control—surrogate models, feedback control and objective reduction. Math Comput Appl 2018;23(2):30. https://doi.org/10.3390/mca23020030.

[51] T.J. Bohme and B. Frank, Hybrid systems, optimal control and hybrid vehicles, Adv Ind Control 2017.

[52] Guzzella L, Sciarretta A. *Vehicle Propulsion Systems (Second Edition): Introduction to Modeling and Optimization*. 2nd ed. Berlin, Heidelberg: Springer Berlin Heidelberg; 2007.

[53] M. Ehsani, Y. Gao, and A. Emadi, Modern electric, hybrid electric, and fuel cell vehicles. 2017.

[54] W.L. McCarthy, W.S. Peters, and D.R. Rodger, "Marine diesel power plant practices," T R Bull pp. 3–49, 1990.

[55] Serrao L, et al. Open issues in supervisory control of hybrid electric vehicles: a unified approach using optimal control methods. Oil Gas Sci Technol Rev IFP Energ Nouv 2013;68(1):23–33. https://doi.org/10.2516/ogst/2012080.

[56] Theotokatos G. On the cycle mean value modelling of a large two-stroke marine diesel engine. Proc Inst Mech Eng Part M J Eng Marit Environ 2010;224(3). https://doi.org/10.1243/14750902JEME188.

[57] "ISO - ISO 3046-1:2002 - Reciprocating internal combustion engines — Performance — Part 1: Declarations of power, fuel and lubricating oil consumptions, and test methods — additional requirements for engines for general use." https://www.iso.org/standard/28330.html (accessed Mar. 13, 2023).

[58] Adedipe T, Shafiee M, Zio E. Bayesian network modelling for the wind energy industry: an overview. Reliab Eng Syst Saf 2020;202:107053. https://doi.org/10.1016/j.ress.2020.107053. May.

[59] Amin MT, Khan F, Imtiaz S. Dynamic availability assessment of safety critical systems using a dynamic Bayesian network. Reliab Eng Syst Saf 2018;178:108–17. https://doi.org/10.1016/j.ress.2018.05.017. Oct.

[60] Bobbio A, Portinale L, Minichino M, Ciancamerla E. Improving the analysis of dependable systems by mapping fault trees into Bayesian networks. Reliab Eng Syst Saf 2001;71(3). https://doi.org/10.1016/S0951-8320(00)00077-6.

[61] Ji C, Su X, Qin Z, Nawaz A. Probability analysis of construction risk based on noisy-or gate Bayesian networks. Reliab Eng Syst Saf 2021;217:107974. https://doi.org/10.1016/j.ress.2021.107974. July2022.

[62] L. BayesFusion, "SMILE: structural modeling, inference, and learning engine." Accessed: Oct. 17, 2021. [Online]. Available: https://www.bayesfusion.com/smile/.

[63] GeNIe, "GeNIe modeler user manual," 2020.

[64] Cox DR. Regression models and life-tables. J R Stat Soc Ser B 1972;34(2). https://doi.org/10.1111/j.2517-6161.1972.tb00899.x.

[65] Jardine AKS, Ralston P, Reid N, Stafford J. Proportional hazards analysis of diesel engine failure data. Qual Reliab Eng Int 1989;5(3). https://doi.org/10.1002/qre.4680050305.

[66] Technology Society SINTEF, Author, Author Norges Teknisk-naturvitenskapelige Universitet, DNV GL OREDA...: Offshore and Onshore Reliability Data Handbook.6th ed, 2015.

[67] Tsoumpris C, Theotokatos G. Performance and reliability monitoring of ship hybrid power plants. J ETA Marit Sci 2022;10(1):29–38. https://doi.org/10.4274/jems.2022.82621. Mar.

[68] Denson WK, Rome Laboratory (Griffiss Air Force Base NY). *Nonelectronic parts reliability data 1991*. Reliability Analysis Center; 1991.

[69] Chiachío J, Jalón ML, Chiachío M, Kolios A. A Markov chains prognostics framework for complex degradation processes. Reliab Eng Syst Saf 2019;195:106621. https://doi.org/10.1016/j.ress.2019.106621. January2020.

[70] Wang J, Miao Y. Optimal preventive maintenance policy of the balanced system under the semi-Markov model. Reliab Eng Syst Saf 2021;213:107690. https://doi.org/10.1016/j.ress.2021.107690. April.

[71] Scania, "Operator's manual DI16 EMS with S6/PDE marine engine.".

[72] Elbert P, Ebbesen S, Guzzella L. Implementation of dynamic programming for n-dimensional optimal control problems with final state constraints. IEEE Trans Control Syst Technol 2013;21(3):924–31. https://doi.org/10.1109/TCST.2012.2190935.

[73] Sundström O, Guzzella L. A generic dynamic programming Matlab function. Proc IEEE Int Conf Control Appl 2009;(7):1625–30. https://doi.org/10.1109/CCA.2009.5281131.

[74] Kim S, Kim NH, Choi JH. A study toward appropriate architecture of system-level prognostics: physics-based and data-driven approaches. IEEE Access 2021;9(2): 157960–72. https://doi.org/10.1109/ACCESS.2021.3129516.
[75] Utne IB, Rokseth B, Sørensen AJ, Vinnem JE. Towards supervisory risk control of autonomous ships. Reliab Eng Syst Saf 2018;196:106757. https://doi.org/10.1016/j.ress.2019.106757. June2020.
[76] Aizpurua JI, Catterson VM, Papadopoulos Y, Chiacchio F, Urso DD. Supporting group maintenance through prognostics-enhanced dynamic dependability prediction. Reliab Eng Syst Saf 2017;168:171–88. https://doi.org/10.1016/j.ress.2017.04.005. April.
[77] Su C, Chen HJ. A review on prognostics approaches for remaining useful life of lithium-ion battery. IOP Conf Ser Earth Environ Sci 2017;93(1). https://doi.org/10.1088/1755-1315/93/1/012040.
[78] Hu Y, Miao X, Si Y, Pan E, Zio E. Prognostics and health management: a review from the perspectives of design, development and decision. Reliab Eng Syst Saf 2021;217:108063. https://doi.org/10.1016/j.ress.2021.108063. September2022.
[79] Rosewater DM, Copp DA, Nguyen TA, Byrne RH, Santoso S. Battery energy storage models for optimal control. IEEE Access 2019;7:178357–91. https://doi.org/10.1109/ACCESS.2019.2957698.
[80] Khorasgani H, Biswas G, Sankararaman S. Methodologies for system-level remaining useful life prediction $. Reliab Eng Syst Saf 2016;154:8–18. https://doi.org/10.1016/j.ress.2016.05.006.